Coupled Inductor Based Non-Isolated High Conversion Ratio Boost Extender

Vikas Kumar Rathore, *Student Member*, *IEEE,* Michael Evzelman,*Member*, *IEEE* and Mor Mordechai Peretz, *Member*, *IEEE*

The Center for Power Electronics and Mixed-Signal IC, Department of Electrical and Computer Engineering
Ben-Gurion University of the Negev, P.O. Box 653, Beer-Sheva, 8410501 Israel
rathore@post.bgu.ac.il, evzelman@bgu.ac.il ,morp@bgu.ac.il
http://www.ee.bgu.ac.il/~pemic

2023 IEEE Applied Power Electronics Conference and Exposition (APEC) | 978-1-6654-7539-6/23/$31.00 ©2023 IEEE | DOI: 10.1109/APEC43580.2023.10131533

***Abstract* – A coupled inductor based non-isolated boost extender with high conversion ratio is presented. The topology features higher power density due to the lower physical inductor cores count, with similar efficiency and component stresses as a conventional boost extender. Topology analysis, and its suitability for multiple extension inductor coupling is shown, coupling coefficient impact on the converter performance, and a short design guide is presented. An analysis and design of coupled inductor is demonstrated, and experimental prototype of 200W is developed and tested in the laboratory. The experimental prototype operated at maximum efficiency of 94.4% providing step up conversion ratio of 10.5, employing a coupled inductor the size of a single inductor of the conventional boost extender converter. The theoretical predictions were found to be in a good agreement with experimental results.**

Keywords –High density, coupled inductor, boost extender, Capacitor stacking, High voltage gain, Single-switch, Switched capacitor.

I. INTRODUCTION

A high step-up DC-DC converters are popular as an interface converter in many industrial applications such as photovoltaic (PV) applications, back-up energy systems for an uninterruptible power supplies, and telecommunication industry [1]-[3]. The conventional boost converter is considered for commercial and industrial applications due to its compact structure and good efficiency at lower conversion ratios. However due to parasitic losses, high voltage and current stress across the switch, boost converter doesn't provide a sufficient performance at extreme duty cycles for high voltage gain applications [4]-[5]. To achieve high conversion ratio at low duty cycles many step up techniques, such as switch capacitor, switch inductor/voltage lift, multistage-level and interleaved structure are available in the literature [6]-[7]. However, the major drawback of switch capacitor and switch inductor/voltage lift techniques, is that increased current stresses across the switches typical for these techniques, increase the losses and degrade the converter efficiency. In the recent years, coupled inductor-based boost topologies are being revisited, and some new topologies are proposed to alleviate the limitations caused by operation with high duty cycle [8]-[9]. The major downside of the coupled inductor approach is the leakage inductance, which causes a high current spike and high voltage stress across the switches. An active and passive clamp snubber circuits [10]-[11] are used to suppress the voltage spikes across the switch is one possible remedy. There are some other classic converters that employ magnetic coupling [12]-[16] (CUK, SEPIC) and provide higher conversion ratios at lower duty cycles. These converters utilize coupled inductor to reduce the size, weight, and losses of the converter. The major advantage of coupling the inductor or integrated magnetic structure is that it gives higher energy storage density [17] compared to independent inductors. In addition, coupling of inductances on a common magnetic core enables to manage current ripple of the coupled inductors, where the current ripple of one of the inductors can be significantly reduced [18].The impact of coupling coefficient is analyzed in conventional coupled inductor based Cuk converter [19]-[21] in which the correlation between the coupling coefficient and size of coupling capacitor is addressed.

The idea of boost extenders as discussed in this study, is based around introducing a voltage source in series with the boost as shown in Fig. 1(a). The added voltage sources in the regular boost converter can be realized by using the series capacitors C_s, Fig. 2(b). In order to provide continuous charging current I_{cs} to series capacitors an additional charging circuit is added consisting of auxiliary inductor L_2, auxiliary capacitors C_1, and a diode D_1, Fig. 2(c). This novel generic approach of stacking multiple series capacitor fundamental cells is shown in Fig. 1(d). Each fundamental cell consists of an inductor, series capacitor, auxiliary capacitor and a diode. In this article the stacked capacitors C_1, C_2, C_3 are referred as auxiliary capacitors, and the series capacitors C_{s1}, C_{s2}, C_{s3} are called series capacitors. The innovation of this study is an introduction of a coupled inductor into the boost extending circuitry, to increase power density of the converter, with no penalties to the efficiency, output voltage ripple, or component stresses. The unique architecture of the boost extender enables to achieve equal volt-second balance across all the extending stage inductors, which in turn enables to wind these inductors all on the same core. The objective of this work is to evaluate the new boost extender topology with coupled inductor instead of multiple separate inductors, validate the criteria for inductor coupling of the extending stages, analyze the coupling coefficients on the converter performance, and present some design outlines of the topology.

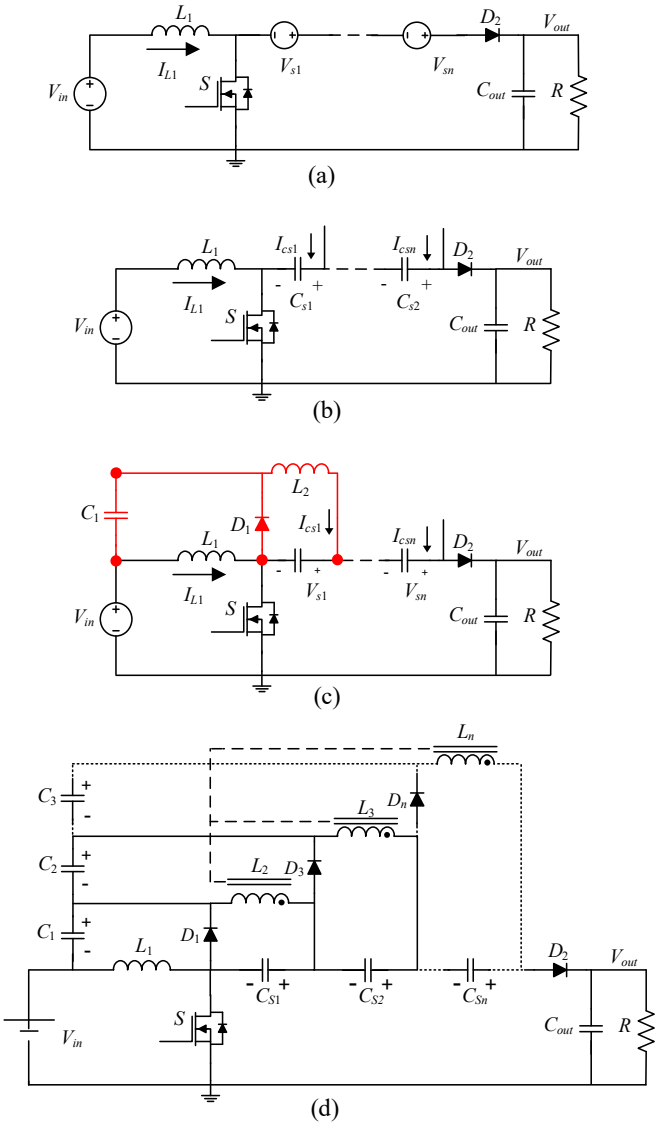

Fig. 1. Development of coupled inductor-based Boost Extender Topology.

The rest of the article is organized as follows: Section II presents coupled inductors approach for boost extending topology, section III focuses on effect of coupling on boost extender topology performance, section IV outlines some design guides of the coupled inductor-based converter, section V demonstrates the experimental results, and conclusions are drawn in section VI.

II. COUPLED INDUCTOR APPROACH FOR BOOST EXTENDER CONFIGURATION

The general boost extender with coupled inductor is shown in Fig. 1(d). To analyze the boost extender topology with coupled inductor two stacked capacitor modules are considered Fig. 2. The converter has two operation modes [22] Continuous Conduction Mode (CCM) and Continuous Bidirectional Conduction Mode (CBCM).

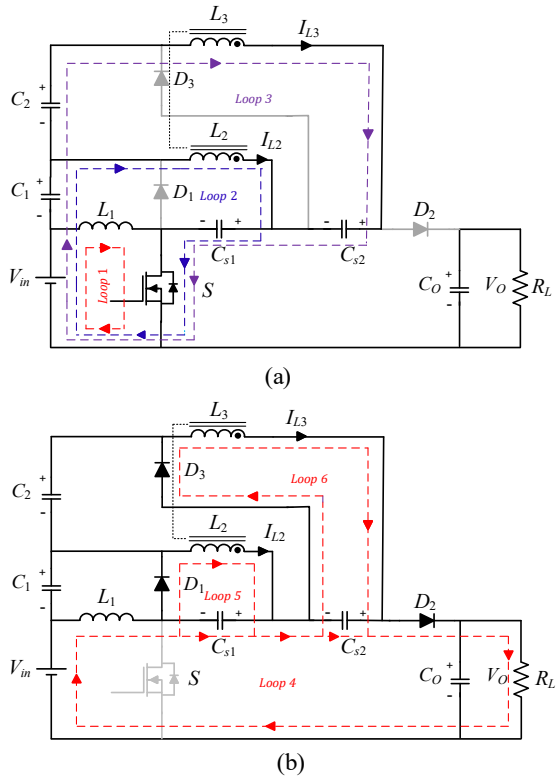

Fig. 2. Coupled inductor-based boost extender high voltage gain topology states: (a) Switch On state; (b) Switch Off state.

The operation mode is decided based on auxiliary inductor currents I_{L2} and I_{L3}. When these currents are all time positive, converter operation is considered to be in CCM mode. If, however, the currents are changing direction, and become negative at least for part of the switching cycle, converter operation is considered to be in CBCM mode. The two operation stages and conduction loops are identical for both CCM and CBCM modes.

To evaluate whether the conditions on the candidate inductors L_2 and L_3 are suitable for coupling, voltage-balance on the primary inductor L_1 and auxiliary inductors L_2, and L_3 are derived for two conduction states of the converter, Fig. 2a for on time of the switch, and Fig. 2b for the off time of the switch, and are summarized in Eq. 1-3.

$$V_{in}.DT = V_{C1}(1-D)T \tag{1}$$

$$(V_{in} + V_{C1} - V_{CS1}).DT = V_{Cs1}(1-D)T \tag{2}$$

$$(V_{in} + V_{C1} + V_{C2} - V_{Cs1} - V_{Cs2}).DT = V_{Cs2}(1-D)T \tag{3}$$

Following above short analysis, the voltage stresses in all auxiliary and switched capacitors are found to be equal, and as a result the voltages across all the inductors are equal as well [22].

By manipulating above equations, we reach:

When the switch is On, $\{ 0 < t \le DT \}$

$$V_{L2} = V_{L3} = V_{Ln} = V_{in} \tag{a}$$

When switch in Off, $DT < t \le (1-D)T$

$$V_{L2} = V_{L3} = V_{Ln} = V_{in}\frac{D}{1-D} \quad \text{(b)}$$

Using the equal voltages (Equation a and b) and the operation principle of all the inductors being switched on and off according to the switch S on and off times, the volt-second balance can be observed across all the inductors. This is true for *n* stages with *n* auxiliary inductors, and not only for 2 auxiliary inductors as shown here.

III. Effect of Coupling Inductors on Boost Extender Topology

A. *Effect of Coupling coefficient on auxillary inductors value* :

In boost extender topology the auxiliary inductors have self-inductance value (L_2, L_3---L_n). To explain the effect of coupling inductor here we have considered two auxiliary inductors. The coupling coefficient (K) in terms of self and mutual inductance given by the equation below:

Applying the Volt-Second balance on the primary inductor L_1 (1), auxiliary inductor L_2 (2) and L_3 (3) the following equations have been obtained:

$$K = \frac{L_M}{\sqrt{L_1 L_2}} \quad (4)$$

The voltages across the integrated inductor L_1 and L_2 is equal V_{L1}=V_{L2}.

$$V_{L1} = L_1\frac{di_{L1}}{dt} + L_M\frac{di_{L2}}{dt} \quad (5)$$

$$V_{L2} = L_2\frac{di_{L2}}{dt} + L_M\frac{di_{L1}}{dt} \quad (6)$$

The turns ratio N between two coils is defined by the equation below:

$$N = \frac{V_{L1}}{V_{L2}} = \frac{N_1}{N_2} = \sqrt{\frac{L_1}{L_2}} = \frac{L_M}{KL_2} \quad (7)$$

For boost extender case, it is known that the voltage stress across the auxiliary inductors is same so, by manipulating above equation a generalized expression [23] for ripple current through coupled inductor can be obtained as:

$$\frac{di_{L1}}{dt} = \frac{V_{L2}L_2 - V_{L1}L_M}{L_1L_2 - L_M^{\,2}} = \frac{V_{L1}}{L_1((1-K^2)/(1-K\sqrt{L_1/L_2}))} \quad (8)$$

$$\frac{di_{L2}}{dt} = \frac{V_{L1}L_1 - V_{L2}L_M}{L_1L_2 - L_M^{\,2}} = \frac{V_{L2}}{L_2((1-K^2)/(1-K\sqrt{L_2/L_1}))} \quad (9)$$

It can be observed from equation (8) and (9) that the ripple currents in converter with coupled inductor can be calculated by the effective inductance value determined by coupling coefficient K and turn ratio $\sqrt{L_1/L_2}$. In boost extender case the value of inductance is same to operate in different modes of conductions (CCM and CBCM). The equivalent inductance produced as an effect of coupling are given by the equation below:

$$L_{eq} = L_{L1eq} = L_{L2eq} = L_1\frac{1-K^2}{1-K\sqrt{L_1/L_2}} \quad (10)$$

From above equations, ripple current steering in both inductors can be achieved by properly tuning the coupling coefficient K and turn ratio $\sqrt{L_1/L_2}$. Also, with coupling incorporate the required value of effective inductance is reduced compared to self-inductances.

B. *Impact of coupling on ripple current* :

In a coupled inductor design due to finite energy transferring between capacitance, losses in the converter and inductor windings resistances there would be a slight difference in the drive voltage waveform across the windings. Consequently, due to differential voltage lead to a small residual ripple current. To analyses ripple current impact equivalent circuit and model [24] for ripple is shown in Fig. 3. The equivalent leakage inductance is calculated by considering Fig. 3(a):

$$L_{lke} = \left(\frac{N_2}{N_1}\right)^2 (L_M \parallel L_{lk1}) + L_{lk2} = \left(\frac{L_{lk1}+L_M}{L_M}\right)^2 (L_M \parallel L_{lk1}) + L_{lk2} \quad (11)$$

$$L_{lke} = \left(\frac{L_{lk1}+L_M}{L_M}\right)L_{lk1} + L_{lk2} \quad (12)$$

In high leakage coupled inductors, the leakage inductances are usually small compared to the magnetizing inductance L_M (<30%) [24], hence the equivalent leakage inductance can be written as:

$$L_{lke} = L_{lk1} + L_{lk2} \quad (13)$$

From the above model of coupled inductor Fig. 3(b), it is clear that any mismatch in the two-driving voltages appear directly across the effective leakage inductance (L_{lke}). To obtain small current ripple, at least one of the input or output leakage inductance should be large. The ripple current is inversely proportional to the effective leakage of coupled inductor. For tightly coupled inductors, where $K \approx 1$, the leakage between inductors is minimal and ripple current will be high. However, in the boost extender case where we require to wound multiple windings on a single magnetic core, we can neglect the zero-ripple condition.

To illustrate the condition, a simulation has been carried out in OrCAD PSpice (Fig. 4) by considering V_i=20, D=0.75, f_s=100kHz, V_o=200V and self-inductance value of both coupled inductors is selected to be 135µH. It is shown that the ripple across the auxiliary and series capacitors get increased once we reach K values of 0.98. Also, Low load values is used to record and demonstrate (Fig. 5) the both auxiliary coupled inductors current in CBCM mode for two different value of coupling coefficient K.

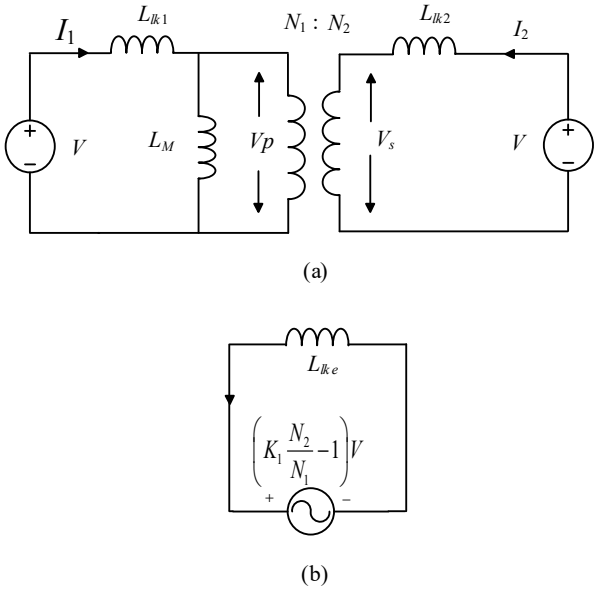

Fig. 3. Coupled inductor model: (a) Equivalent circuit; (b) Ripple derivation model.

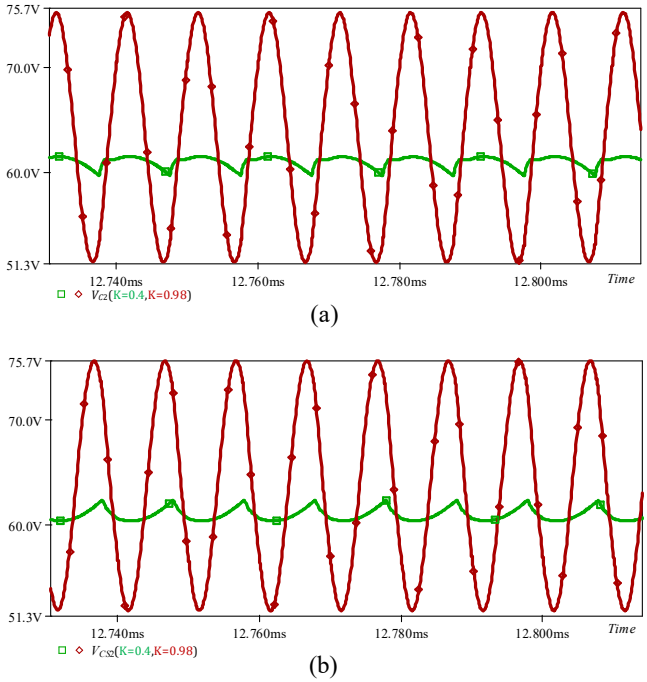

Fig. 4. Simulation results - Ripple voltage waveform recorded under light load condition (CBCM). V_{in} =20V, f=100kHz, D=75% and C_{aux}=C_s=1µF: (a) Auxiliary capacitor, C_2; (b) Series capacitor, C_{s2}. Large ripple (red trace) – high k value, k = 0.98; low ripple (green traces) – Low k value, k = 0.4.

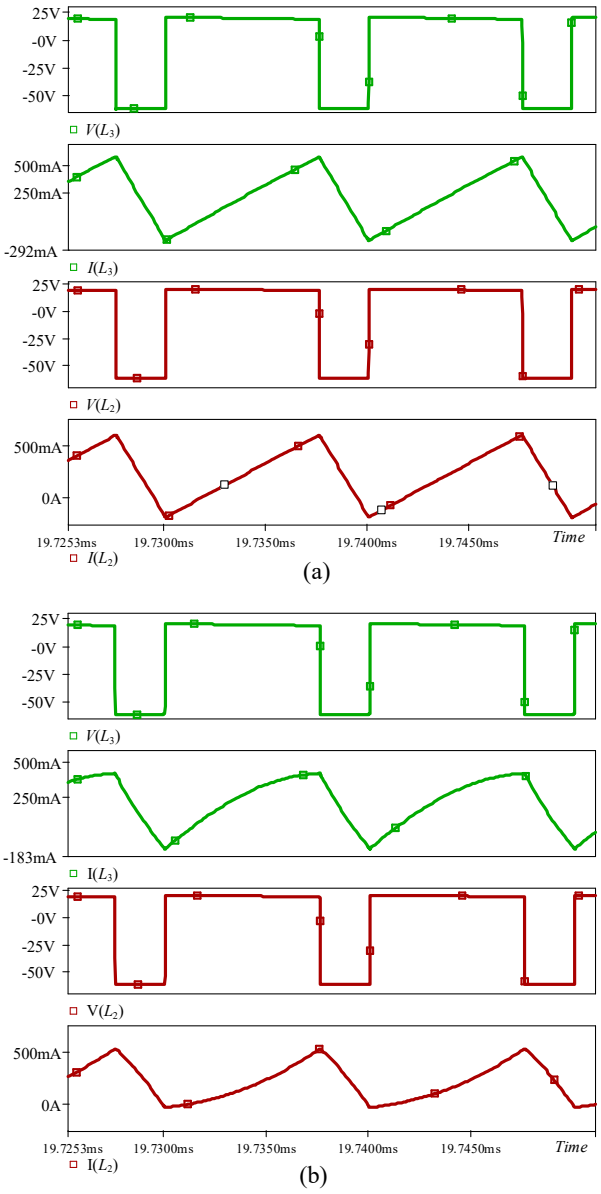

Fig. 5. Simulation results - Inductors waveform recorded under light load condition (CBCM). V_{in} =20V, f=100kHz, D=75% and C_{aux}=C_s=10µF: Auxiliary Inductors voltages, (V_{L3}, V_{L2}) and current waveforms, (I_{I2}, I_{I3}), (a) K=0.4, (b) K=0.98

IV. Design Methodology for Coupled Inductor

This section deals with the design analysis of the coupled inductor that can be used to evaluate the boost extender topology. There are several literatures have been reported [25]-[30] where the coupled inductor is designed for numerous topologies like Multi phase buck, SEPIC and Cuk converter. By considering the limiting parameters like temperature rise due to AC and DC windings losses and saturation limit of core a short design guideline of coupled inductor is explained in this section. The main specification of coupled inductor is shown in Table I.

A. *Selection of core size* :

The selection of the core size is facilitated by calculation of A_p (Area product) required by the application. Most of the manufacturers described it as $A_w.A_e$ .At high frequencies the core losses dominate hence it cannot be operated anywhere near saturation flux density. Whereas at low frequency, core size is dictated by I^2R losses generated by the inductor windings and saturation flux density of the core material. A_p calculation is dependent on operating frequency f, saturation limit of magnetic flux density B_{max} and K_W window factor. The A_p calculation can be described as:

$$A_P = \frac{LI_{pk}I_{rms}}{B_{\max}JK_W} \tag{14}$$

For coupled inductor case an appropriate ferrite core (3F3) is selected. To limit the saturation limit and core losses in ferrite. Maximum flux density of 100mT is chosen for designing coupled inductor.

TABLE I. PARAMETERS FOR COUPLED INDUCTOR DESIGN

Parameter	***Value/Type***
Coupled inductors (L_2, L_3)	135µH, 135µH,
Max Peak current	2A
Max Total Full load current	1A

Using the above parameters and considering window area K_W =0.5, current density J=4.2A/mm^2 in this case, the A_p for the design is found to be 0.68cm^4. An E-core is selected to reduce the overall sizing of coupled inductor. The calculated A_p compared with different E core and it is found that Ferroxcube ETD 34 is suitable for our application.

B. *Calculation of number of turns* :

The next step is to calculate the minimum number of turns that will take the core to B_{max} (Magnetic flux density) at the peak current limit. The number of turns for each inductor can be calculated by using the expression:

$$n_{\min} = \frac{LI_{pk}}{B_{\max}A_e} \tag{15}$$

B_{max} and A_e are the properties of core. In this case maximum magnetic flux density 100mT is chosen for 3F3 core material having effective area is 97mm^2. From design consideration peak current from auxiliary inductor I_{pk} =2A is chosen. By solving the above equation with all parameters, the no. of turns needed for 135 μH single inductor is 28. Using the minimum no. of turns the next step is to find the air length required to get the desired inductance value. The air gap for the inductor design can be calculated by using the equation given below:

$$l_g = \frac{\mu_o\mu_r N^2 A_e}{L}.10^{-2}\,cm \tag{16}$$

By using the above obtained parameters, the both windings of coupled inductor are wounded on the middle leg of E core by inserting calculated air gap of 0.7cm.

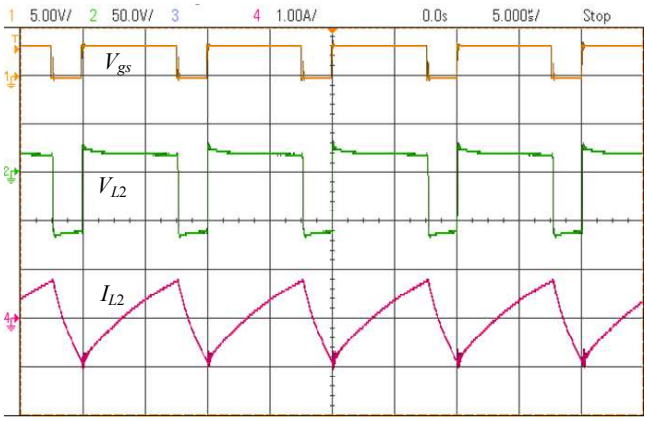

(a)

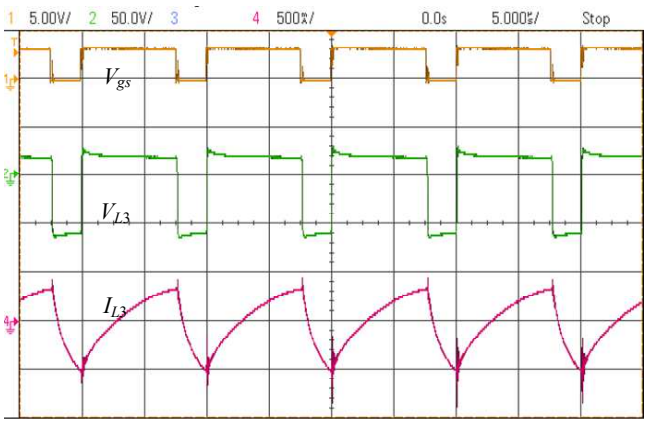

(b)

Fig. 6. Gate signal V_{gs}, Coupled Inductor Voltage (V_{L2}, V_{L3}) and Current (I_{L2}, I_{L3}). Top trace is V_{gs} with 5V/Div; Middle trace is inductor voltage (50V/Div); Bottom trace: (a) I_{L2}, (b) I_{L3} with 1A/Div and 500mA/Div, Time base is 5us/div.

V. EXPERIMENTAL RESULTS

To evaluate the theoretical predictions and the operation of a boost extender with coupled magnetics, a boost extender with two auxiliary inductors L_2 and L_3 on a single magnetic core is build and tested in the laboratory. The specification of the components used for prototype are given in Table II. The power rating of the designed converter is 200W and an output voltage of 208V.

To record the key waveform of converter the input voltage is set to be 20V, and the output was recorder to be 208.83V. The switching frequency was set to 99.9kHz, and the power level was recorded to be 100W. The waveforms are presented for tightly coupled inductors by considering coupling coefficient of K =0.98 in both mode of operation CBCM (Fig .6) and CCM (Fig .7). Also, a lower coupling coefficient having large leakage inductance is considered to record the waveform (Fig .9) in CBCM mode for both auxiliary inductors. As outlined in [20]-[21] the current waveform for tightly coupled inductors diverge from straight triangular form and becomes curved. The efficiency of the boost extender prototype over a wide range of output is tested and demonstrated in Fig .8. A maximum efficiency of 94.4% in CBCM mode was achieved at a power level of 120W.

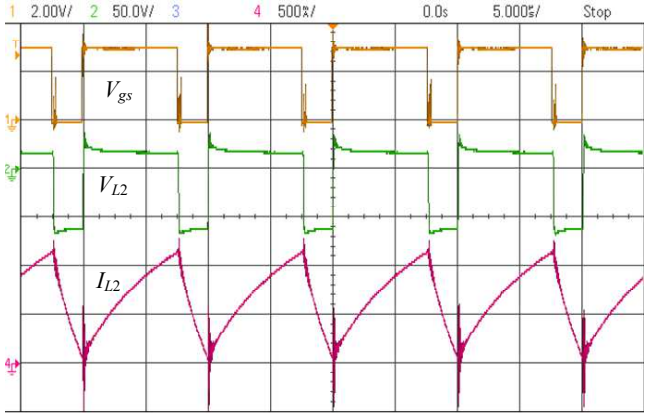

(a)

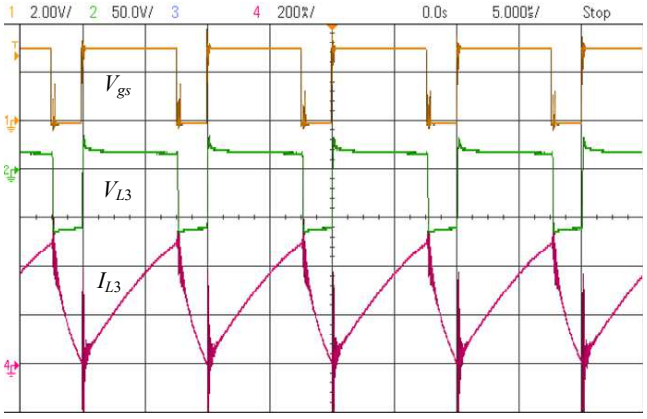

(b)

Fig. 7. Gate signal V_{gs}, Coupled Inductor Voltage (V_{L2}, V_{L3}) and Current (I_{L2}, I_{L3}). Top trace is V_{gs} with 2V/Div; Middle trace is inductor voltage (50V/Div); Bottom trace: (a) I_{L2}, (b) I_{L3} with 500mA/Div and 200mA/Div , Time base is 5us/div.

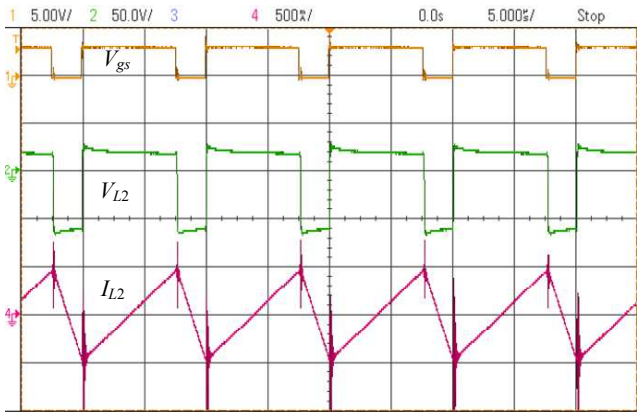

(a)

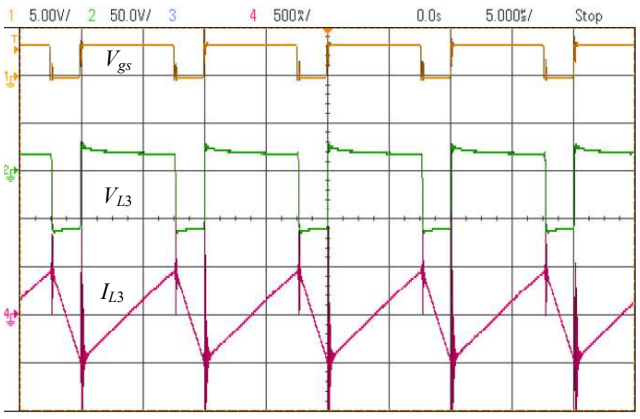

(b)

Fig. 9. Gate signal V_{gs}, Loosely coupled Inductor Voltage (V_{L2}, V_{L3}) and Currents (I_{L2}, I_{L3}). Top trace is V_{gs} with 5V/Div; Middle trace is inductor voltage (50V/Div); Bottom trace: (a) I_{L2}, (b) I_{L3} with 500mA/Div, Time base is 5us/div.

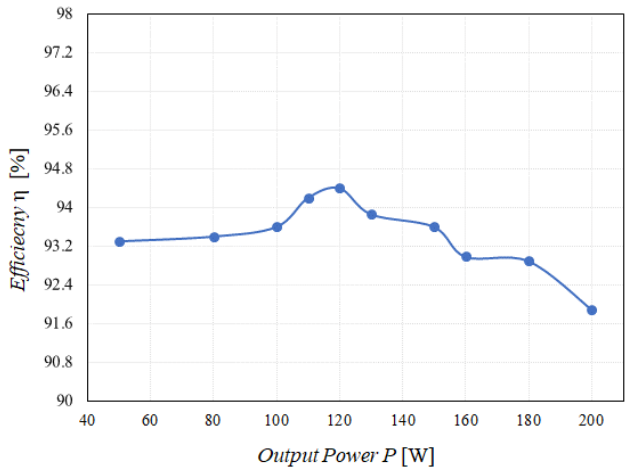

Fig. 8. Experimental efficiency Curves under CBCM mode when V_{in}=20V and V_{out} =208V

TABLE II. EXPERIMENTAL PARAMETERS

Input voltage V_{in}	20 V
Output voltage V_o	208 V
Output Power P_o	200W
Switching Frequency f_o	100KHz
Primary Inductors L_1	100 µH
Magnetizing Inductance L_2, L_3	135.23 µH, 135.23µH
Leakage Inductance L_2, L_3	2.21 µH
Coupling Coefficient (K)	0.98
Capacitors C_{s1}, C_{S2}	20 µF, 20 µF
Capacitors C_1, C_2	15 µF, 15 µF
Diodes	V40PW22CHM3/I
Main Switch	IXFH120N30X3

VI. CONCLUSION

A boost extender converter using coupled inductor is presented. A boost extender approach is compatible with coupling multiple of its extension inductors on the same single core. This unique approach of single magnetic structure facilitates to reduce size, and weight, while maintaining the

same voltage stress of the components and similar efficiency compared with the uncoupled case of boost extender switching converter.

The experimental prototype with two extension stages attains maximum efficiency of 94.4% at the input voltage of 20V and output voltage of 208V. The experimental waveforms follow to simulation waveforms at different values of coupling coefficients. Theoretical predictions were found to be in a good agreement with experimental results. The converter finds its application in medium voltage boosting such as renewable energy, datacenters, telecom centers and microgrids.

ACKNOWLEDGMENT

This research was supported by the ISRAEL SCIENCE FOUNDATION grant number 2186/19.

REFERENCES

[1] F. Blaabjerg, Z. Chen and S. B. Kjaer, "Power electronics as efficient interface in dispersed power generation systems," in *IEEE Transactions on Power Electronics*, vol. 19, no. 5, pp. 1184-1194, Sept. 2004, doi: 10.1109/TPEL.2004.833453.

[2] O. Abutbul, A. Gherlitz, Y. Berkovich and A. Ioinovici, "Step-up switching-mode converter with high voltage gain using a switched-capacitor circuit," in *IEEE Transactions on Circuits and Systems I: Fundamental Theory and Applications*, vol. 50, no. 8, pp. 1098-1102, Aug. 2003, doi: 10.1109/TCSI.2003.815206.

[3] I. Barbi and R. Gules, "Isolated DC-DC converters with high-output voltage for TWTA telecommunication satellite applications," in *IEEE Transactions on Power Electronics*, vol. 18, no. 4, pp. 975-984, July 2003, doi: 10.1109/TPEL.2003.813762.

[4] Qun Zhao and F. C. Lee, "High-efficiency, high step-up DC-DC converters," in *IEEE Transactions on Power Electronics*, vol. 18, no. 1, pp. 65-73, Jan. 2003, doi: 10.1109/TPEL.2002.807188.

[5] Tseng K. C., Liang T. J, "Novel high-efficiency step-up converter", *IEE Proceedings -Electric Power Applications*, Volume 151, Issue 2,2004, p. 182-190

[6] M. Forouzesh, Y. P. Siwakoti, S. A. Gorji, F. Blaabjerg and B. Lehman, "Step-Up DC–DC Converters: A Comprehensive Review of Voltage-Boosting Techniques, Topologies, and Applications," in *IEEE Transactions on Power Electronics*, vol. 32, no. 12, pp. 9143-9178, Dec. 2017, doi: 10.1109/TPEL.2017.2652318.

[7] Y. Zheng, W. Xie and K. M. Smedley, "A Family of Interleaved High Step-Up Converters with Diode–Capacitor Technique," in *IEEE Journal of Emerging and Selected Topics in Power Electronics*, vol. 8, no. 2, pp. 1560-1570, June 2020, doi: 10.1109/JESTPE.2019.2907691.

[8] R. J. Wai, C. -Y. Lin, R. -Y. Duan and Y. -R. Chang, "High-Efficiency DC-DC Converter with High Voltage Gain and Reduced Switch Stress," in *IEEE Transactions on Industrial Electronics*, vol. 54, no. 1, pp. 354-364, Feb. 2007, doi: 10.1109/TIE.2006.888794.

[9] S. Chen et al., "Research on topology of the high step-up boost converter with coupled inductor," *IEEE Trans. Power Electron.*, vol. 34, no. 11, pp. 10733–10745, Nov. 2019.

[10] T. F. Wu, Y. S. Lai, J. C. Hung and Y. M. Chen, "Boost Converter with Coupled Inductors and Buck-Boost Type of Active Clamp," 2005 *IEEE 36th Power Electronics Specialists Conference*, 2005, pp. 399-405, doi: 10.1109/PESC.2005.1581655.

[11] B. Gu, J. Dominic, B. Chen, L. Zhang and J. -S. Lai, "Hybrid Transformer ZVS/ZCS DC–DC Converter with Optimized Magnetics and Improved Power Devices Utilization for Photovoltaic Module Applications," in *IEEE Transactions on Power Electronics*, vol. 30, no. 4, pp. 2127-2136, April 2015, doi: 10.1109/TPEL.2014.2328337.

[12] S. Ćuk and Zhe Zhang, "Coupled-inductor analysis and design," 1986 *17th Annual IEEE Power Electronics Specialists Conference*, 1986, pp. 655-665, doi: 10.1109/PESC.1986.7415621.

[13] D. Maksimovic, R. W. Erickson and C. Griesbach, "Modeling of cross-regulation in converters containing coupled inductors," in *IEEE Transactions on Power Electronics*, vol. 15, no. 4, pp. 607-615, July 2000, doi: 10.1109/63.849030.

[14] W. Martinez, J. Imaoka, Y. Itoh, M. Yamamoto and K. Umetani, "Analysis of coupled-inductor configuration for an interleaved high step-up converter," 2015 *9th International Conference on Power Electronics and ECCE Asia (ICPE-ECCE Asia)*, 2015, pp. 2241-2248, doi: 10.1109/ICPE.2015.7168088.

[15] A. Ajami, H. Ardi and A. Farakhor, "A Novel High Step-up DC/DC Converter Based on Integrating Coupled Inductor and Switched-Capacitor Techniques for Renewable Energy Applications," in *IEEE Transactions on Power Electronics*, vol. 30, no. 8, pp. 4255-4263, Aug. 2015, doi: 10.1109/TPEL.2014.2360495.

[16] X. Hu and C. Gong, "A High Voltage Gain DC–DC Converter Integrating Coupled-Inductor and Diode–Capacitor Techniques," in *IEEE Transactions on Power Electronics*, vol. 29, no. 2, pp. 789-800, Feb. 2014, doi: 10.1109/TPEL.2013.2257870.

[17] Y. Itoh, S. Kimura, J. Imaoka and M. Yamamoto, "Inductor loss calculation of coupled inductors for high power density boost converter," 2014 *International Power Electronics Conference (IPEC-Hiroshima 2014 - ECCE ASIA)*, 2014, pp. 2497-2502, doi: 10.1109/IPEC.2014.6869940.

[18] S.Cuk, "Switching dc-to-dc converter with zero input or output current ripple, "in *IEEE Ind Appl.Soc.Annu.Meeting*, 1978 Record,pp.1131-1145, (IEEE Publication 78CH1346-61A).

[19] E. Santi and S. Cuk, "Comparison and design of three coupled inductor structures," Proceedings of IECON'94 - *20th Annual Conference of IEEE Industrial Electronics*, 1994, pp. 262-267 vol.1, doi: 10.1109/IECON.1994.397786.

[20] G. Di Capua and N. Femia, "A Critical Investigation of Coupled Inductors SEPIC Design Issues," in *IEEE Transactions on Industrial Electronics*, vol. 61, no. 6, pp. 2724-2734, June 2014, doi: 10.1109/TIE.2013.2274419.

[21] L.H. Dixon, "High Power Factor Preregulator Using the SEPIC Converter," *Unitrode seminar SEM900*, Topic 6, 1993.

[22] V. K. Rathore, M. Evzelman and M. M. Peretz, "Non-Isolated High Conversion Ratio Boost Extender Based on Back-end Series Capacitor Stacking," 2022 IEEE 23rd *Workshop on Control and Modeling for Power Electronics (COMPEL)*,2022, pp. 1-7, doi: 10.1109/COMPEL53829.2022.9829993.

[23] Prabhu, P. and Urundady, V. (2020), Design of coupled inductors using split winding scheme for bridgeless SEPIC. *IET Power Electronics*, 13: 1434-1444. https://doi.org/10.1049/iet-pel.2019.1227

[24] Zhang, Z.: 'Coupled-inductor magnetics in power electronics', *California Institute of Technology*, 1987

[25] L.H. Dixon, "Coupled Inductor Design," *Unitrode Seminar* SEM900, Topic 8, 1993.

[26] G. Zhu, B. McDonald and K. Wang, "Modeling and Analysis of Coupled Inductors in Power Converters," 2009 *Twenty-Fourth Annual IEEE Applied Power Electronics Conference and Exposition*, 2009, pp. 83-89, doi: 10.1109/APEC.2009.4802637.

[27] A. F. Witulski, "Introduction to modeling of transformers and coupled inductors," in IEEE *Transactions on Power Electronics*, vol. 10, no. 3, pp. 349-357, May 1995, doi: 10.1109/63.388001.

[28] S. Cuk, "New magnetic structures for switching converters," in *IEEE Transactions on Magnetics*, vol. 19, no. 2, pp. 75-83, March 1983, doi: 10.1109/TMAG.1983.1062239.

[29] Liang, D. and Shin, H.-B. (2019) "Coupled Inductor Design Method for 2-Phase Interleaved Boost Converters," *Journal of Power Electronics . Korean Society of Power Electronics*, 19(2), pp. 344–352. doi: 10.6113/JPE.2019.19.2.344.

[30] J. Imaoka and M. Yamamoto, "A novel integrated magnetic structure suitable for transformer-linked interleaved boost chopper circuit," 2012 *IEEE Energy Conversion Congress and Exposition (ECCE)*, 2012, pp. 3279-3284, doi: 10.1109/ECCE.2012.6342339.